ECE

WEMPEC

Wisconsin Electric Machines and Power Electronics Consortium

RESEARCH REPORT
84-7

A Rotor Parameter Identification Scheme for Vector Controlled Induction Motor Drives

T. Matsuo
Mitsubishi Electric Co.
Kobe, Japan

T.A. Lipo
University of Wisconsin
Madison, Wisconsin

Department of Electrical and Computer Engineering
University of Wisconsin-Madison
Madison, Wisconsin 53706

June 1984

A Rotor Parameter Identification Scheme for Vector-Controlled Induction Motor Drives

TAKAYOSHI MATSUO AND THOMAS A. LIPO, SENIOR MEMBER, IEEE

Abstract—A rotor parameter identification technique for the purpose of updating the control gains of an induction motor vector controller is described. The approach utilizes the current source nature of a current-regulated PWM inverter by injecting a prescribed negative sequence current perturbation signal. The corresponding negative sequence voltage is sensed and decomposed into its d and q components. By injecting the signal at two widely separated frequencies (one perhaps dc), it is shown that the rotor resistance can be uniquely derived. Verification of the validity of the technique is obtained by a full-scale simulation of a vector controlled induction motor drive.

INTRODUCTION

VECTOR CONTROL techniques incorporating microprocessors have made possible the application of induction motor drives in high-performance applications where only dc motor drives were previously available. In general, two generic types of vector control, sometimes called field-oriented control, are in use. The first scheme, developed by Blaschke [1] and shown in Fig. 1(a), is probably the most accurate induction motor control method available. This technique utilizes direct sensing of the air gap flux vector by use of Hall probes, search coils, or other measurement techniques. The measured air gap flux signal is fed back to the control and used to decouple the torque producing component of stator current from the flux producing component. Since this method uses feedback control and direct sensing of the regulated variable, it is essentially insensitive to variations in motor parameters (i.e., plant parameters).

The second method, shown in Fig. 1(b) and originally devised by Hasse [2], is an indirect flux sensing method wherein the rotor flux is estimated from the stator current vector, voltage vector, and/or rotor speed, and then this estimate is, in effect, fed forward to the flux and torque controller. As is true for any feedforward technique, this approach is much more sensitive to errors in parameters and the rotor resistance, rotor leakage inductance as well as magnetizing inductance must be accurately known to achieve performance equivalent to Blaschke's method.

Paper IPCSD 84-37, approved by the Industrial Drives Committee of the IEEE Industry Applications Society for presentation at the 1984 Industry Applications Society Annual Meeting, Chicago, IL, April 3–6, 1984. Manuscript released for publication September 11, 1984. This work was supported in part by the Mitsubishi Electric Corporation and in part by the Wisconsin Electric Machines and Power Electronics Consortium.

T. Matsuo was with the Department of Electrical and Computer Engineering, University of Wisconsin—Madison, 1415 Johnson Drive, Madison, WI 53706. He is now with Mitsubishi Electric Corporation, Power and Industrial Systems Center, Wadasaki-cho, Kyogo-ku, Kobe, Japan.

T. A. Lipo is with the Department of Electrical and Computer Engineering, University of Wisconsin, 1415 Johnson Drive, Madison, WI 53706.

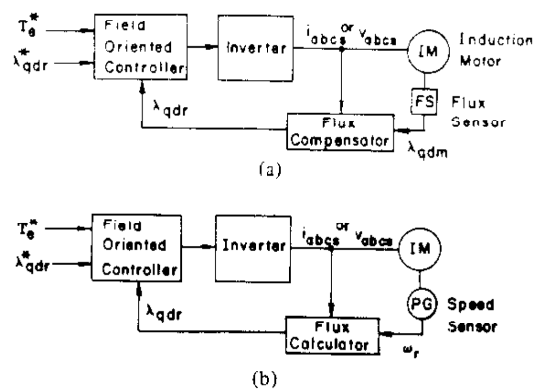

Fig. 1. Two generic types of induction motor vector control systems. (a) Direct flux sensing method. (b) Indirect flux sensing method.

While the direct method is inherently the most desirable control scheme, it suffers from high cost and the unreliability of the flux measurement. Although the indirect method can approach the performance of the direct measurement scheme, the major weakness of this approach is centered upon the accuracy of the control gains which, in turn, depend heavily on the motor parameters assumed in the feedforward control algorithm. Unfortunately, motor parameters change widely with temperature, frequency, and current amplitude. Hence inaccuracy in setting the control gains often leads to saturation or underexcitation of the machine resulting in a corresponding deterioration in the dynamic performance, particularly with large machines. Recently, much attention has been given to the possibility of identifying these changes of motor parameters while the drive is in normal operation [3], [4].

Vector control principles can be applied without regard to the type of inverter, and VVI (voltage source six step), CSI (current source), and pulsewidth modulated (PWM) voltage source inverters as well as cycloconverters have been used as the frequency converter. However, the recent activity in the development of high-power bipolar transistors, as well as other power switches which have led to high-power devices with inherent turn-off as well as turn-on capabilities, has made the so-called current-regulated PWM inverter the widespread choice in fast response ac servo applications [4]–[6]. This approach employs a fast-switching PWM inverter to control the current supplied to the motor on an almost instantaneous basis. The inverter appears as nearly an ideal current source to the motor provided that the switching of the inverter power devices is sufficiently fast relative to the frequency desired.

The ability to inject currents into the motor with a current source has opened up new possibilities for parameter determi-

0093-9994/85/0500-0624$01.00

nation. In particular, test signals can be superimposed upon the nominal torque-producing components of current while the motor drive is in actual operation. This paper describes a new identification technique utilizing injected negative sequence components. It is shown that the stator as well as rotor resistance and leakage inductance can be determined on line while the motor is driving the load. The theory is verified with a full-scale hybrid computer simulation of a field-oriented controlled PWM inverter. induction motor drive. Computer test results are studied from a realistic 175-hp machine in which the rotor resistance is varied over an eight to one range. Good correlation with theory is obtained.

INDUCTION MACHINE REPRESENTATION FOR VECTOR CONTROL

The dynamic behavior of a three-phase three-wire induction motor with a squirrel-cage rotor or a short-circuited wound rotor can be conveniently described by vector equations in a d-q rotating reference frame. With the appropriate constraints, the d-q frame can be made to rotate synchronously with the stator or rotor voltage, current or flux vectors. The so-called field coordinate systems are obtained when the d-q frame rotates synchronously with the magnetic field (magnetic flux) within the machine. It is useful for purposes of motor control to allow the reference frame to rotate synchronously with the rotor flux vector (rotor field coordinates). If the angular velocity ω_e is used to represent the instantaneous angular speed of the rotor flux vector, then the equations which describe the transient behavior of an induction motor can be written as [7], [8]

$$\mathbf{v}_{qds}{}^e=\left[r_s+L_s\left(\frac{d}{dt}+\boldsymbol{\omega}_e\times\right)\right]\mathbf{i}_{qds}{}^e+L_m\left(\frac{d}{dt}+\boldsymbol{\omega}_e\times\right)\mathbf{i}_{qdr}{}^e \tag{1}$$

and

$$0=L_m\left[\frac{d}{dt}+(\boldsymbol{\omega}_e-\boldsymbol{\omega}_r)\times\right]\mathbf{i}_{qds}{}^e+\left\{r_r{}'+L_r{}'\left(\frac{d}{dt}+(\boldsymbol{\omega}_e-\boldsymbol{\omega}_r)\times\right)\right\}\mathbf{i}_{qdr}{}^e \tag{2}$$

$$\mathbf{T}_e=\frac{3}{2}\frac{P}{2}L_m\mathbf{i}_{qdr}{}^e\times\mathbf{i}_{qds}{}^e \tag{3}$$

$$\mathbf{T}_e-\mathbf{T}_L=\frac{2}{P}J\frac{d\boldsymbol{\omega}_r}{dt}. \tag{4}$$

In these equations the boldfaced quantities are three-dimensional Cartesian vectors which without a zero-sequence component, can be considered as rotating on the d-q plane [8]. With no zero sequence, the stator d-q voltage vector is given as

$$\mathbf{v}_{qds}{}^e=[v_{qs}{}^e,\ v_{ds}{}^e,\ 0]^t. \tag{5}$$

The superscript t in (5) denotes the vector transpose, and the superscript e signifies that the vector is represented in a synchronously rotating reference frame which is, in this case, rotating synchronously with the rotor flux vector. Note that in (5) provision is made for a third zero-sequence component $v_{ns}{}^e$. However, this term has been set to zero since only a three-wire system will be considered.

The corresponding stator and rotor d-q current vectors are

$$\mathbf{i}_{qds}{}^e=[i_{qs}{}^e,\ i_{ds}{}^e,\ 0]^t \tag{6}$$

$$\mathbf{i}_{qdr}{}^e=[i_{qr}{}^e,\ i_{dr}{}^e,\ 0]^t. \tag{7}$$

The angular velocity vector of the flux vector is

$$\boldsymbol{\omega}_e=[0,\ 0,\ \omega_e]^t. \tag{8}$$

In addition, the following symbols are defined:

- r_s stator resistance,
- $r_r{}'$ rotor resistance (referred to the stator),
- L_m stator/rotor mutual inductance,
- L_s stator self-inductance,
- $L_r{}'$ rotor self-inductance (referred to the stator),
- ω_r equivalent two pole rotor mechanical angular velocity,
- T_e electromagnetic torque,
- T_L load torque,
- P number of poles,
- J total moment of inertia of the drive.

The transformation from the physical three-phase stationary variables to two-phase rotating variables is readily accomplished by means of the following equations:

$$\mathbf{v}_{qds}=\frac{2}{3}\begin{bmatrix}\cos\omega_e t & \cos(\omega_e t-2\pi/3) & \cos(\omega_e t+2\pi/3)\\ \sin\omega_e t & \sin(\omega_e t-2\pi/3) & \sin(\omega_e t+2\pi/3)\\ 0 & 0 & 0\end{bmatrix}\begin{bmatrix}v_{as}\\ v_{bs}\\ v_{cs}\end{bmatrix} \tag{9}$$

$$\mathbf{i}_{qds}=\frac{2}{3}\begin{bmatrix}\cos\omega_e t & \cos(\omega_e t-2\pi/3) & \cos(\omega_e t+2\pi/3)\\ \sin\omega_e t & \sin(\omega_e t-2\pi/3) & \sin(\omega_e t+2\pi/3)\\ 0 & 0 & 0\end{bmatrix}\begin{bmatrix}i_{as}\\ i_{bs}\\ i_{cs}\end{bmatrix} \tag{10}$$

where v_{as}, v_{bs}, v_{cs} are the three phase stator voltages and i_{as}, i_{bs}, i_{cs} are the three stator phase currents. An equation similar to (9) applies for the transformation of rotor currents except that the angular frequency ω_e is replaced by the slip angular frequency $\omega_s = \omega_e - \omega_r$.

The rotor flux vector $\boldsymbol{\lambda}_{qdr}{}^e$ in the synchronously rotating reference frame can be written in terms of the stator and rotor d-q current vectors as

$$\boldsymbol{\lambda}_{qdr}{}^e=L_m\mathbf{i}_{qds}{}^e+L_r{}'\mathbf{i}_{qdr}{}^e. \tag{11}$$

The stator current vector $\mathbf{i}_{qds}{}^e$ can be expressed in terms of the rotor flux vector $\boldsymbol{\lambda}_{qdr}{}^e$, the slip angular frequency vector $\boldsymbol{\omega}_s$, and the induction motor parameters by eliminating the rotor current vector $\mathbf{i}_{qdr}{}^e$ from (2) using (11). The result is

$$\mathbf{i}_{qds}{}^e=\frac{1}{L_m}\boldsymbol{\lambda}_{qdr}{}^e+\frac{L_r{}'}{L_m r_r{}'}\frac{d}{dt}\boldsymbol{\lambda}_{qdr}{}^e+\frac{L_r{}'}{L_m r_r{}'}\boldsymbol{\omega}_s\times\boldsymbol{\lambda}_{qdr}{}^e. \tag{12}$$

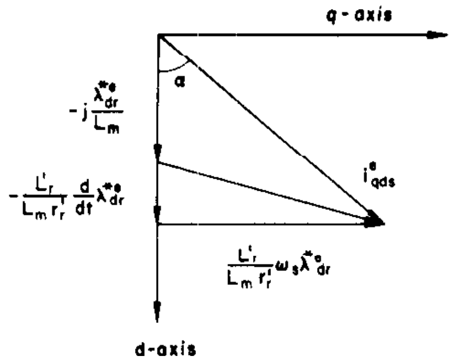

Fig. 2. Vector diagram of stator current and rotor flux linkage in synchronously rotating reference frame.

Fig. 2 shows the resulting vector diagram of the stator current in the synchronously rotating reference frame for the particular case where the d axis is aligned with the rotor flux vector. Note that, in this case, the rotor flux vector λ_{qdr}^e has only one nonzero component $-\lambda_{dr}^e$. The d and q components of the stator current vector thereby reduce to the following:

$$i_{qs}^e = \frac{L_r'}{L_m r_r'} \omega_s \lambda_{dr}^e \tag{13}$$

$$i_{ds}^e = \frac{1}{L_m} \lambda_{dr}^e + \frac{L_r'}{L_m r_r'} \frac{d}{dt} \lambda_{dr}^e. \tag{14}$$

The electrical angle between the stator current and rotor flux vectors is

$$\alpha = \tan^{-1} \frac{i_{qs}^e}{i_{ds}^e}. \tag{15}$$

The electromagnetic torque can now be expressed in terms of only the q component of the stator current vector i_{qs}^e and the d component of the rotor flux vector λ_{dr}^e as

$$T_e = \frac{3}{2}\frac{P}{2}\frac{L_m}{L_r'} \lambda_{dr}^e i_{qs}^e. \tag{16}$$

Note that (16) has the same form as the torque equation of a dc machine. Hence it is a key result since it implies that control strategies similar to that employed for dc machines can be used to control an induction motor. In particular, shunt dc motor principles can be adapted to induction motor control wherein the electromagnetic torque and the rotor flux are controlled independently by regulating the d and q components of stator current together with slip frequency using the following relationships obtained from (13), (14), and (16),

$$i_{qs}^{e*} = \frac{4}{3P}\frac{L_r'}{L_m}\frac{T_e^*}{\lambda_{dr}^{e*}} \tag{17}$$

$$i_{ds}^{e*} = \frac{1}{L_m} \lambda_{dr}^{e*} + \frac{L_r'}{L_m r_r'} \frac{d}{dt} \lambda_{dr}^{e*} \tag{18}$$

$$\omega_s^* = \frac{4}{3P} r_r' \frac{T_e^*}{(\lambda_{dr}^{e*})^2} \tag{19}$$

where T_e^* and λ_{dr}^{e*} are the desired values of torque and rotor flux. In these equations the asterisk denotes the commanded value of the variable. The rotor slip frequency ω_s can only be controlled indirectly by means of the PWM inverter. The necessary stator frequency command to the inverter can be obtained by simply summing the commanded slip frequency with the measured rotor frequency (i.e., speed).

$$\omega_e^* = \omega_r + \omega_s^*. \tag{20}$$

While (17)–(20) are sufficient to define the input conditions to the motor, the stator current commands in the synchronously rotating reference frame $i_{qds}^{e*} = [i_{qs}^{e*}, i_{ds}^{e*}, 0]'$ must now be converted to the stationary reference frame since the stator current of the induction motor can only be controlled by a static inverter in the stationary reference frame. The stator current command in the stationary reference frame i_{qds}^{s*} can be obtained by the inverse transformation to (10) where the commanded values of stator current replace the actual values. That is,

$$\begin{bmatrix} i_{as}^* \\ i_{bs}^* \\ i_{cs}^* \end{bmatrix} = \begin{bmatrix} \cos \omega_e^* t & \sin \omega_e^* t & 0 \\ \cos(\omega_e^* t - 2\pi/3) & \sin(\omega_e^* t - 2\pi/3) & 0 \\ \cos(\omega_e^* t + 2\pi/3) & \sin(\omega_e^* t + 2\pi/3) & 0 \end{bmatrix} i_{qds}^*. \tag{21}$$

A configuration for field-oriented control of an induction motor implementing (17)–(20) is shown in Fig. 3. Note that the set points for the stator current and frequency are obtained without benefit of a flux measurement. Hence the so-called indirect vector control scheme has been realized. In Fig. 3 the overall vector controller generates instantaneous three-phase current commands i_{as}^*, i_{bs}^*, and i_{cs}^* from the torque command T_s^* and the rotor flux command λ_{dr}^{e*} and a speed feedback signal. The d-q coordinate stator current commands in the synchronously rotating reference frame i_{qs}^{e*} and i_{ds}^{e*} and the slip frequency command ω_s^* are obtained from the torque command T_e^* and the rotor flux command λ_{dr}^{e*} according to (17)–(19). For simplicity, the transformation of current commands from the synchronous to the stationary from is done in a two-stage process. First, the corresponding d-q coordinate stator current commands in the stationary reference frame i_{qds}^{s*} are obtained by changing coordinates from the synchronously rotating reference frame to the stationary reference frame. The stationary d-q coordinate stator current command is then transformed to three-phase current commands. A static PWM inverter is subsequently used to realize the desired three-phase currents in the induction motor.

INFLUENCE OF ROTOR RESISTANCE CHANGE ON CONTROL PERFORMANCE

It is apparent from the foregoing discussion that field-oriented control is only effective so long as the values of the motor parameters in the controller are in agreement with the actual motor parameters. If errors exist, the decoupling condition cannot be achieved. Interactions would arise and the control performance deteriorates so that it is useful to access the severity of this change. The machine performance during

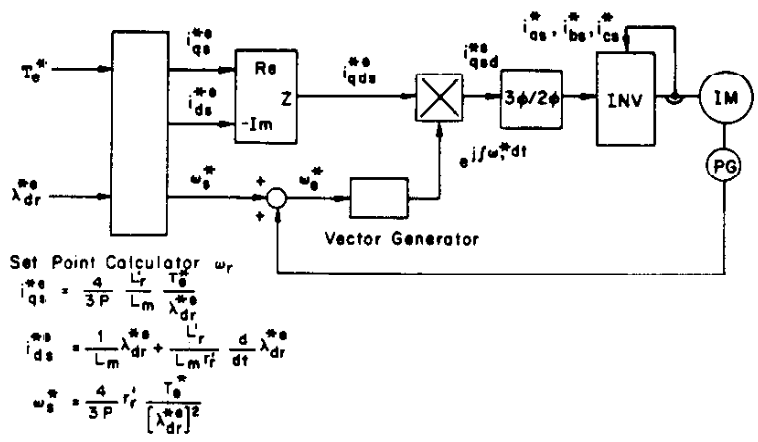

Fig. 3. Configuration for indirect field-oriented control.

steady state is readily obtained in the synchronously rotating reference frame from (2) if we simply set the time derivatives to zero:

$$0 = L_m(\omega_e - \omega_r) \times i_{qds}{}^e + [r_r' + L_r'(\omega_e - \omega_r) \times] i_{qdr}{}^e. \tag{22}$$

Since a 90° counterclockwise rotation in the d-q plane corresponds to a phase rotation of $+90°$ in the corresponding steady-state phasor, (22) is equivalent to the phasor (complex variable) expression

$$0 = j\omega_s{}^* L_m \tilde{i}_{qds}{}^{e*} + (r_r' + j\omega_s{}^* L_r')\tilde{i}_{qdr}{}^e \tag{23}$$

where, in the steady state $\tilde{i}_{qds}{}^e = \tilde{i}_{qds}{}^{e*}$ and $\omega_s = \omega_s{}^*$, the commanded values of stator current and angular slip frequency. In addition, $\tilde{i}_{qds}{}^{e*}$ represents the complex phasor equivalent of the vector $i_{qds}{}^{e*}$ and since the d axis is oriented clockwise to the q axis in the d-q plane,

$$\tilde{i}_{qds}{}^{e*} = i_{qs}{}^{e*} - j i_{ds}{}^{e*}.$$

A similar interpretation is now given the other d-q variables.

Using (13) and (14) specialized to the steady state, this expression can be written as

$$\tilde{i}_{qds}{}^{e*} = \frac{L_r'}{L_m r_r'} \omega_s{}^* \lambda_{dr}{}^{e*} - j \frac{\lambda_{dr}{}^{e*}}{L_m}. \tag{24}$$

If the value of the rotor resistance of the field-oriented controller coincides with the actual value, it can be readily shown that the actual rotor flux and electromagnetic torque indeed coincides with the commanded values of rotor flux and torque.

It is useful to consider now the effect on regulation if the actual rotor resistance changes to $r_r' + \Delta r_r'$ due to a variation of temperature, slip frequency or saturation. As a result, from (23)

$$\begin{aligned}\tilde{\lambda}_{qdr}{}^e &= L_m \tilde{i}_{qds}{}^{e*} + L_r' \tilde{i}_{qdr}{}^e \\ &= L_m \tilde{i}_{qds}{}^{e*} + L_r'\left(-\frac{j\omega_s{}^* L_m}{r_r' + \Delta r_r' + j\omega_s{}^* L_r'} \tilde{i}_{qds}{}^{e*}\right) \\ &= \left(L_m - \frac{j\omega_s{}^* L_m L_r'}{r_r' + \Delta r_r' + j\omega_s{}^* L_r'}\right)\left(\frac{L_r' \omega_s{}^*}{L_m r_r'} - \frac{j}{L_m}\right) \lambda_{dr}{}^{e*}\end{aligned}$$

or, equivalently,

$$\tilde{\lambda}_{qdr} = \Delta\lambda_{qr}{}^e - j(\lambda_{dr}{}^{e*} + \Delta\lambda_{dr}{}^e) \tag{25}$$

where

$$\Delta\lambda_{qr}{}^e = \frac{(K_r - 1)(K_r r_r' \omega_s{}^* L_r')}{(K_r r_r')^2 + (\omega_s{}^* L_r')^2} \lambda_{dr}{}^{e*} \tag{26}$$

$$\Delta\lambda_{dr}{}^e = \frac{(K_r - 1)(\omega_s{}^* L_r')^2}{(K_r r_r')^2 + (\omega_s{}^* L_r')^2} \lambda_{dr}{}^{e*} \tag{27}$$

in which we have defined

$$r_r' + \Delta r_r' = K_r r_r'. \tag{28}$$

The actual torque with incorrect setting of the rotor resistance is expressed as the following

$$T_e = \frac{3}{2} \frac{P}{2} \frac{L_m}{L_r'} \lambda_{qdr}{}^e \times i_{qds}{}^{e*}$$

or

$$T_e = T_e{}^* + \Delta T_e \tag{29}$$

where

$$\Delta T_e = \frac{3}{2} \frac{P}{2} \frac{L_m}{L_r'} (\Delta\lambda_{dr}{}^e i_{qs}{}^{e*} - \Delta\lambda_{qr}{}^e i_{qs}{}^{e*}). \tag{30}$$

Fig. 4 shows the resulting flux deviation due to the variation of the rotor resistance. It can be observed that underexcitation will occur if the actual rotor resistance is smaller than the value of the rotor resistance set in the field-oriented controller,and overexcitation will occur if the actual rotor resistance is larger than the value in the controller. A ±20-percent variation of rotor resistance causes about a ±20-percent error in the rotor field excitation. The variation of the rotor flux vector due to rotor resistance change is shown in Fig. 5. Note that the rotor flux vector widely varies due to the change of the rotor resistance.

The torque deviation due to variation of rotor resistance is shown in Fig. 6 A ±20-percent variation of the rotor resistance again causes about a ±20-percent deviation from

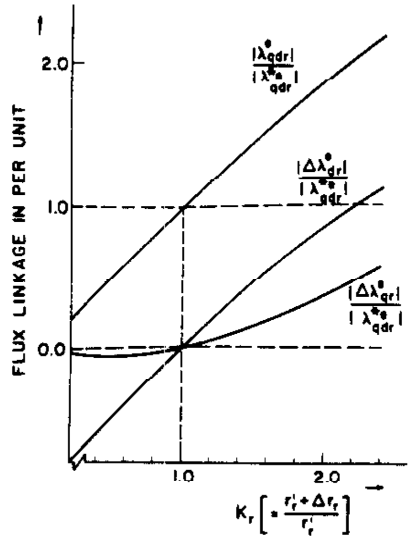

Fig. 4. Rotor flux deviation due to variation of rotor resistance.

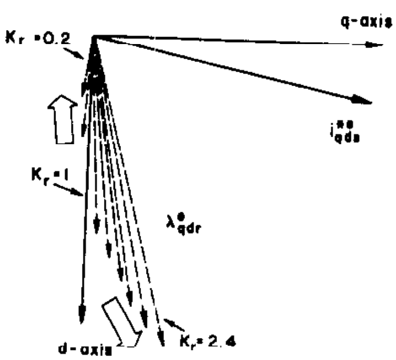

Fig. 5. Rotor flux spatial variation due to change in rotor resistance.

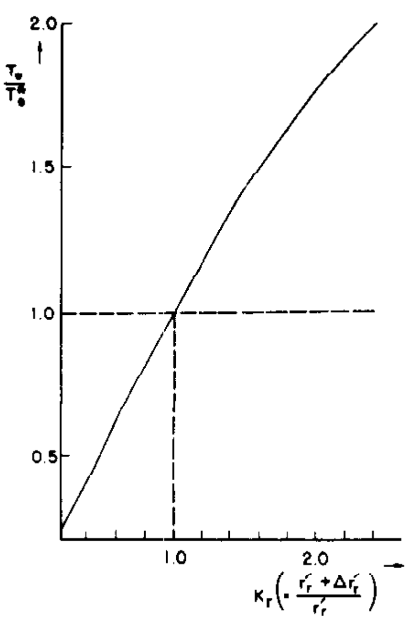

Fig. 6. Torque deviation resulting from variation of rotor resistance.

the expected torque value. The induction motor parameters in the Appendix have been used for this calculation. It is apparent that it is useful to provide for some means of determining the rotor resistance or the rotor time constant if motor saturation or underexcitation is to avoided.

ROTOR RESISTANCE IDENTIFICATION

An identification method for the rotor resistance of the induction motor is now described. The technique enables the field-oriented controller to correct the set point of the rotor resistance in the controller when the actual value of the resistance is changed. The identification of the rotor resistance is achieved by injecting a negative sequence current, detecting the negative sequence voltage, and calculating the value of the rotor resistance from the obtained information.

The equations of an induction motor with a squirrel-cage rotor expressed in a reference frame which is rotating negatively at an angular frequency $-\omega_n$ can be described by the following expressions which can be derived from the general equations of the induction motor:

$$v_{qds}{}^{n} = \left[r_s + L_s\left(\frac{d}{dt} - \omega_n \times\right)\right] i_{qds}{}^{n} + L_m\left(\frac{d}{dt} - \omega_n \times\right) i_{qdr}{}^{n} \tag{31}$$

$$0 = L_m\left[\frac{d}{dt} - (\omega_n + \omega_r)\times\right] i_{qds}{}^{n} + \left\{ r_r' + L_r'\left(\frac{d}{dt} - (\omega_n + \omega_r)\times\right)\right\} i_{qdr}{}^{n} \tag{32}$$

where $v_{qds}{}^{n}$, $i_{qds}{}^{n}$, and $i_{qdr}{}^{n}$ stator voltage, stator current, and rotor current vectors respectively, expressed in the negative sequence reference frame.

Let us now define $v_{qds}{}^{en}$, $i_{qds}{}^{en}$, and $i_{qdr}{}^{en}$ as the components of $v_{qds}{}^{n}$, $i_{qds}{}^{n}$, and $i_{qdr}{}^{n}$, respectively, which rotate synchronously with the negative sequence frame. Hence $v_{qds}{}^{en}$, $i_{qds}{}^{en}$, and $i_{qdr}{}^{en}$ have only dc components which can be related to phasor components corresponding to the negative sequence. The following steady-state equations can then be derived from (31) and (32):

$$\tilde{v}_{qds}{}^{en} = (r_s - j\omega_n L_s)\tilde{i}_{qds}{}^{en} - j\omega_n L_m \tilde{i}_{qdr}{}^{en} \tag{33}$$

$$0 = -j(\omega_n + \omega_r)L_m \tilde{i}_{qds}{}^{en} + [r_r' - j(\omega_n + \omega_r)L_r']\tilde{i}_{qdr}{}^{en}. \tag{34}$$

Equations (33) and (34) imply following four scalar equations:

$$v_{qs}{}^{en} = r_s i_{qs}{}^{en} - \omega_n L_s i_{ds}{}^{en} - \omega_n L_m i_{dr}{}^{en} \tag{35}$$

$$v_{ds}{}^{en} = \omega_n L_s i_{qs}{}^{en} + r_s i_{ds}{}^{en} + \omega_n L_m i_{qr}{}^{en} \tag{36}$$

$$0 = -(\omega_n + \omega_r)L_m i_{ds}{}^{en} + r_r' i_{qr}{}^{en} - (\omega_n + \omega_r)L_r' i_{dr}{}^{en} \tag{37}$$

$$0 = -(\omega_n + \omega_r)L_m i_{qs}{}^{en} - r_r' i_{dr}{}^{en} - (\omega_n + \omega_r)L_r' i_{qr}{}^{en}. \tag{38}$$

These four equations suggest that if negative sequence currents $i_{qs}{}^{en}$ and $i_{ds}{}^{en}$ are injected into the control system and the negative sequence voltages $v_{qs}{}^{en}$ and $v_{ds}{}^{en}$ are detected, or if negative sequence voltages are injected and the negative sequence currents are detected, the rotor resistance r_r' and the stator resistance r_s can be obtained in terms of i_{qs}^{en}, i_{ds}^{en}, v_{qs}^{en}, v_{ds}^{en}, L_m, L_r', L_s, ω_r, and ω_n.

From (36)–(38) the following equation can be obtained for the d axis component of stator voltage:

$$\left[\frac{r_r'^2}{(\omega_n+\omega_r)^2 L_r'^2}+1\right] v_{ds}^{en} = \left\{\left[\frac{r_r'^2}{(\omega_n+\omega_r)^2 L_r'^2}+1\right]\omega_n L_s - \frac{L_m^2}{L^r}\omega_n\right\} i_{qs}^{en} + \frac{\omega_n}{(\omega_n+\omega_r)}\frac{L_m^2}{L_r'^2} r_r' i_{ds}^{en} + \left[\frac{r_r'^2}{(\omega_n+\omega_r)^2 L_r'^2}+1\right] r_s i_{ds}^{en}. \tag{40}$$

The injected negative sequence current components i_{qs}^{en} and i_{ds}^{en} can be chosen arbitrarily. Upon choosing $i_{qs}^{en} = 0$ and using the valid approximation

$$r_r'^2 \ll (\omega_n+\omega_r)^2 L_r'^2, \tag{41}$$

(40) reduces to

$$v_{ds}^{en} = r_s i_{ds}^{en} + \frac{\omega_n}{(\omega_n+\omega_r)}\frac{L_m^2}{L_r'^2} r_r' i_{ds}^{en}. \tag{42}$$

In similar fashion the q axis voltage equation (35) reduces to

$$v_{qs}^{en} = \omega_n\left[L_s - \frac{L_m'^2}{L_r}\right] i_{ds}^{en*}. \tag{43}$$

Equations (42) and (43) can be used to detect both the stator and rotor resistances as well as the total motor leakage reactance. The resistance r_r' can be measured by injecting the same negative sequence current amplitude i_{ds}^{en*} twice at the different negative sequence frequencies ω_{n1} and ω_{n2} and sensing the negative sequence voltages v_{ds}^{en1} and v_{ds}^{en2}, respectively:

$$v_{ds}^{en1} = r_s i_{ds}^{en*} + \frac{\omega_{n1}}{(\omega_{n1}+\omega_{r1})}\frac{L_m^2}{L_r'^2} r_r' i_{ds}^{en*} \tag{44}$$

$$v_{ds}^{en2} = r_s i_{ds}^{en*} + \frac{\omega_{n2}}{(\omega_{n2}+\omega_{r2})}\frac{L_m^2}{L_r'^2} r_r' i_{ds}^{en*}. \tag{45}$$

An equation for the calculation of r_r' can be obtained by eliminating r_s from (44) and (45):

$$r_r' = \frac{[v_{ds}^{en1} - v_{ds}^{en2}]}{i_{ds}^{en*}}\frac{L_m^2}{L_r'^2}\left[\frac{\omega_{n1}}{(\omega_{n1}+\omega_{r1})} - \frac{\omega_{n2}}{(\omega_{n2}+\omega_{r2})}\right]^{-1}. \tag{46}$$

If desired, the stator resistance can be found by eliminating r_r' from (44) and (45), whereupon

$$r_s = \left[\frac{1}{i_{ds}^{en*}}\right]\frac{v_{ds}^{en1}\left[\frac{\omega_{n2}}{(\omega_{n2}+\omega_{r2})}\right] - v_{ds}^{en2}\left[\frac{\omega_{n1}}{(\omega_{n1}+\omega_{r1})}\right]}{\frac{\omega_{n2}}{(\omega_{n2}+\omega_{r2})} - \frac{\omega_{n1}}{(\omega_{n1}+\omega_{r1})}}. \tag{47}$$

It is readily shown that if L_{ls} and L_{lr}' denote the stator and rotor leakage inductances, then

$$\left[L_s - \frac{L_m^2}{L_r'}\right] \approx L_{ls} + L_{lr}' \tag{48}$$

and from (43) the sum of the stator plus rotor leakage inductance is therefore

$$L_{ls} + L_{lr}' \approx -\frac{v_{qs}^{en}}{i_{ds}^{en*}}\frac{1}{\omega_n}. \tag{49}$$

Note that an important special case exists if one of the two frequencies is equal to zero (dc component). In this case the stator resistance can be determined directly from (45) as

$$r_s = \frac{v_{ds}^{en2}}{i_{ds}^{en*}} \tag{50}$$

since the frequency ω_{n2} is identically zero. The rotor resistance can now be found from (45) by simply subtracting the stator IR drop from the d axis stator voltage measurement taken at frequency ω_{n1}.

A configuration for implementation of the identification of the rotor resistance is shown in Fig. 7. The negative sequence current reference i_{qds}^{sn*}, which is generated from i_{qds}^{en*} through the coordinate changer, is added to the stator current command i_{qds}^{s*} and converted from two-phase to three-phase variables. The stator currents are controlled by these command signals. The three-phase voltages of the induction motor are detected and changed from three-phase to two-phase system, and the desired negative sequence voltages v_{qs}^{en} and v_{ds}^{en} can be obtained through the coordinate changer and the low-pass filter. The measurement must be done twice for the computation of r_r' and a memory function is required for the r_r' calculator.

ANALOG COMPUTER SIMULATION OF VECTOR CONTROLLED DRIVE

A full-scale analog computer simulation has been carried out to verify the feasibility of the rotor resistance identification method. The overall control system which has been simulated is shown in Fig. 8. In particular, an indirect field-oriented controller and associated slip frequency control using a current regulated voltage source inverter has been implemented. In addition, a negative sequence current injection circuit and negative sequence voltage detector have been added for purposes of rotor resistance identification.

The simulation equations used to represent an induction motor in the stationary reference frame as well as the dc link filter are given in [7] and [9]. Details of the simulation of the vector controller are also given in [9]. The motor parameters used in the simulation are listed in the Appendix.

Fig. 9 shows analog traces of the waveforms of the current command i_{as}*, the motor phase current i_{as}, and the gate pulses of the inverter. While this current control scheme is an excellent one, note that a turn-off time margin, which gives the enough turn-off time to the switch devices such as SCR's or transistors, is required because of the limitation of the turn-off

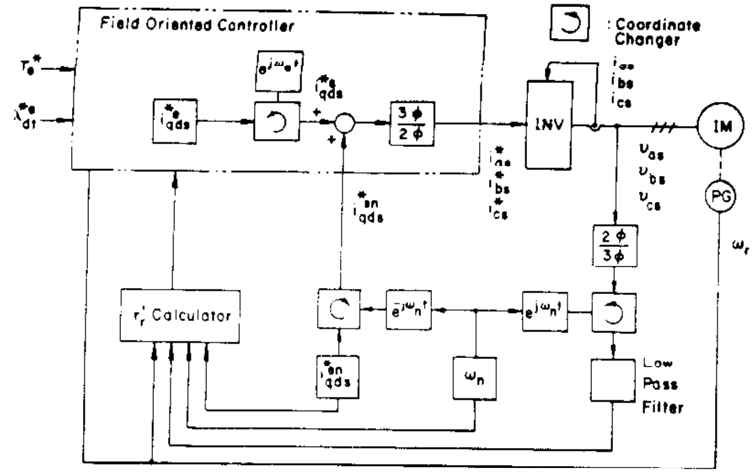

Fig. 7. Configuration for implementation of rotor resistance identification in indirect vector controller.

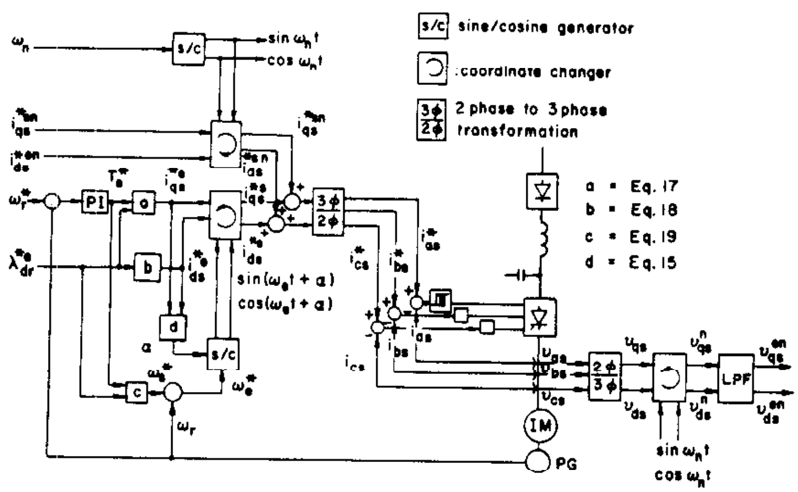

Fig. 8. System simulated on analog computer showing modified vector controller and current regulated PWM inverter.

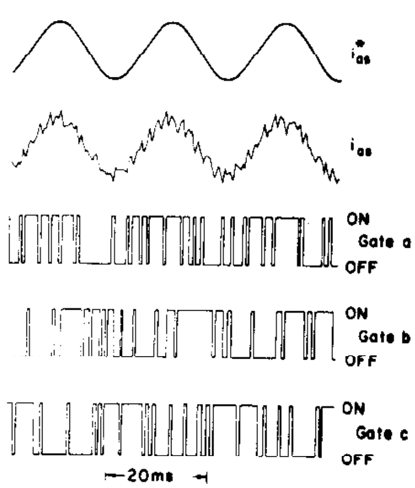

Fig. 9. Computer traces showing current command signal, resulting motor current, and inverter gate pulses.

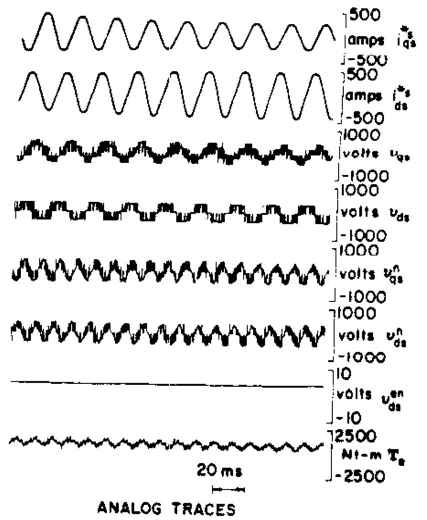

Fig. 10. Analog computer traces illustrating operation of rotor resistance identification circuit $\omega_e = \omega_e^*$.

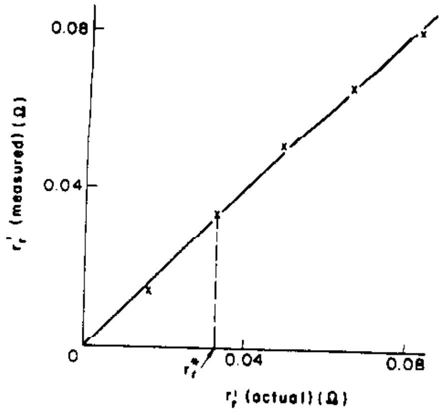

Fig. 11. Comparison of actual and measured rotor resistance r_r' when varied over 8:1 range.

capability of the power devices in the actual system. This practical aspect of inverter design has been neglected in the simulation study.

Fig. 10 shows the voltage waveforms obtained through the negative sequence voltage detection principle, where the negative sequence frequency $\omega_n = \omega_e^*$. Note that injection of a negative sequence current component at the positive sequence frequency simply corresponds to an unbalanced set of input current commands i_{qs}^{*s} and i_{ds}^{*s}. In addition, a strong second harmonic torque pulsation is clearly induced due to the interaction of the positive and negative rotating components of MMF. Some care must clearly be taken to avoid possible mechanical resonances, and the test should be made only for short periods at the required intervals needed to keep the vector controller gains within acceptable bounds. An analog type low-pass filter has been implemented to detect the negative sequence voltage so that it takes about 1 s to obtain the negative sequence voltage and about 2 s to determine the actual rotor resistance of the induction motor. It is apparent that the identification process can be accomplished much more rapidly if the digital filtering is implemented.

Fig. 11 summarizes the simulation results obtained for the identification of the rotor resistance. The simulation was repeated for five different values of the rotor resistance corresponding to 50, 100, 150, 200, and 250 percent of the original value by setting the related potentiometers in the analog computer. The injected negative sequence frequencies, ω_{n1} and ω_{n2} were the rated stator frequency ω_e^* and $1/2\omega_e^*$, respectively. Fig. 11 shows good agreement between the actual values and the measured values of the rotor resistance r_r' which are within plus or minus five percent error.

The difficult point for applying this rotor resistance identification method to the actual drive system is the technique for sensing the dc component of the negative sequence voltage, that is, the dc component of the negative sequence voltage is a very small value compared with the stator voltage. For example, in the case of the induction motor used for this simulation the rated voltage is 270 V rms, whereas the dc component of the d axis negative sequence voltage is 3–4 V. This implies a resolution accuracy on the order of 0.1 percent if good accuracy is to be maintained. Measurement of the leakage reactance of the machine can also be taken periodically, but this parameter does not vary widely with temperature but with load changes so that frequent measurements of this quantity may not be necessary. Resolution accuracy is not so important an issue in this case since the leakage reactance drop is five to ten times larger than the resistive drop.

It is interesting to note that if the commutation time of the inverter is negligible, the waveform of the gate pulses can be considered as simply scaled equivalents of the inverter voltage waveforms. Hence the gate pulses in the current control type voltage source inverter themselves can be used for the negative sequence voltage detection instead of detecting the actual motor voltages. Hence if a microprocessor is used to implement the field-oriented controller, the entire calculation for the rotor resistance identification could be completed within the microprocessor.

CONCLUSION

The vector controlled induction motor drive system is presently considered one of the prime candidates to take the place of dc motor drives. In particular, the *slip frequency* or *indirect* type field-oriented control system is considered to be most practical system because, first, it does not require a flux sensor. Hence it can be applied to induction motor drive systems which are already in operation without flux sensors. Secondly, the approach is readily adapted to utilization of microprocessors.

The performance of the field-oriented control by the slip frequency control method, however, depends heavily upon the accuracy of the induction motor parameters. It has been shown that changes in rotor resistance have a most dominant effect on the control performance. An important requirement to obtain good control performance is to make the motor parameters in the field-oriented controller coincide with the actual parameters of the motor.

An on-line technique for establishing the exact value of the rotor resistance of the induction motor has been described in this paper. Identification of the rotor resistance is achieved by

TABLE I
INDUCTION MOTORS PARAMETERS

Quantity	Symbol	Value
Phase voltage	V_b	270 V rms
Base frequency	ω_b	270.2 rad/s
Stator resistance	r_s	0.0217 Ω
Stator referred rotor resistance	r_r'	0.0329 Ω
Stator leakage reactance	X_{ls}	0.874 Ω
Stator referred rotor leakage reactance	X_{lr}'	0.0996 Ω
Magnetizing reactance	X_m	3.6493 Ω
Total rotational inertia	J	11.4 kg-m^2
Number of poles	P	4

injecting a negative sequence current, detecting the negative sequence voltage and calculating the value of the rotor resistance from the obtained information. The mathematical expressions for this technique have been derived and their validity demonstrated by an analog computer simulation. The technique described in this paper enables the field-oriented controller to correct the value of the rotor resistance in the controller without resorting to a thermal sensor or a thermal machine model.

While computer models are sufficient to establish basic principles, it is, of course, desirable to verify the validity of any proposed technique on an actual drive system. While premature to report here, a program for the practical implementation in hardware of a complete indirect vector controller with on-line parameter determination is presently under way at the University of Wisconsin.

APPENDIX

INDUCTION MOTOR PARAMETERS

Table I shows the parameters of the induction motor used in the analog computer simulation. The rated torque of the machine is 1020 NT·m at 1200 r/min. The resistances and reactances are the conventional per phase equivalent circuit parameters.

REFERENCES

[1] F. Blaschke, "Das Verfahren der Feldorientierung zur Regelung der Drehfeldmachine" ("The method of field orientation for control of three phase machines"), Ph.D. dissertation, TU Braunschweig, 1974.

[2] K. Hasse, "Zur Dynamik Drehzahlgeregelter Antriebe mit Stomrichtergespeisten Asynchron-Kurzschlusslaufermachinen" ("On the dynamics of speed control of static ac drives with squirrel-cage induction machines"), Ph.D. dissertation, TH Darmstadt, 1969.

[3] L. J. Garces, "Parameter adaptation for the speed-controlled static ac drive with a squirrel-cage induction motor," *IEEE Trans. Ind. Appl.*, vol. IA-16, pp. 173–178, 1980.

[4] R. Gabriel and W. Leonhard, "Microprocessor control of induction motor," in *Proc. IEEE/IAS Int. Semiconductor Power Converter Conf.*, 1982, pp. 385–396.

[5] T. Okuyama *et al.*, "High performance ac motor speed control system using GTO converters," *IPEC-Tokyo Conf. Rec.*, 1983, pp. 720–731.

[6] A. B. Plunkett, "A current-controlled PWM transistor inverter drive," in *1979 IEEE-IAS Annu. Meet. Conf. Rec.*, pp. 785–792.

[7] P. C. Krause and C. H. Thomas, "Simulation of symmetrical induction machinery," *IEEE Trans. Power App. Syst.*, vol. PAS-84, pp. 1038–1053, Nov. 1965.

[8] T. A. Lipo, "A Cartesian vector approach to reference frame theory of ac machines," in *Conf. Rec. Int. Conf. Electrical Machines*, Lausanne, Sept. 18–21, 1984.

[9] T. Matsuo and T. A. Lipo, "Hybrid computer simulation of a field oriented induction motor drive," in *Conf. Rec. 5th Brazilian/1st Latin-American Conf. on Automatic Control*, Sept. 3–6, 1984, pp. 273–280.

Takayoshi Matsuo was born in Himeji, Japan, on May 13, 1951. He received the B.S. degree in electrical engineering and the M.E. degree in applied electronics from the Tokyo Institute of Technology, Japan, in 1975 and 1977 and the M.S. degree in electrical engineering from University of Wisconsin, Madison, in 1983.

He joined Mitsubishi Electric Corporation, Japan, in 1977 and has been engaged in development and designing of power converters for motor drive systems.

Thomas A. Lipo (M'64–SM'71), for a photograph and biography, please see page 616 of this issue.